Report on Czech research activities in Petuniabukta, Billefjorden, Svalbard, performed in summer season 2013

RESEARCH ACTIVITIES SVALBARD 2013

Centre for Polar Ecology
University of South Bohemia in České Budějovice
Czech Republic

The research is supported by the grant of Czech Ministry of Education (MSMT) LM2010009 CzechPolar - Czech polar stations: Construction and logistic expenses.

Cover photo: Jan Kavan

2013

1. Introduction

In 2013, we started our seventh season in Petuniabukta, Svalbard. Our research programme followed on previous research project *Biological and Climatic Diversity of the Central Part of the Svalbard Archipelago* (INGO LA341) in 2007-2010 and present project *Czech Polar Stations: Construction and Logistics Expenses* (LM2010009). Major part of the scientific activities was connected with a new project *Creating of Working Team and Pedagogical Conditions for Teaching and Education in the Field of Polar Ecology and Life in Extreme Environment*, reg. No. CZ.1.07/2.2.00/28.0190 co-financed by the European Social Fund and by state budget of the Czech Republic.

As in previous years, we occupied Russian hunting hut at the west coast of Petuniabukta and the containers located in Pyramiden port facility served for storage. Mr. M. Dvořáček documented research activities in field.

For more information visit polar.prf.jcu.cz, please.

2. Season 2013 Research Programme

The field research started on July 1, 2013, and was completed on August 31, 2013. The list of expedition participants and their periods of stay is summarized in Tab. 2.1.

Tab. 2.1. List of expedition participants with their affiliations and their periods of stay. .

	Affiliation(s)	Group	Dates
Alexandra Bernardová	JU	BOTA	01/07-31/08
Jan Blahůt	IRSM	GEO	10/08-13/08
Miloslav Devetter	ISB+JU	ZOO	01/08-23/08
Oleg Dittrich	JU	ZOO	01/08-31/08
Miloslav Dvořáček	JU	photographer	29/07-16/08
Josef Elster	JU+IBOT	MICRO	18/07-16/08
Zbyněk Engel	UK+JU	GEO	04/07-15/07
Tomáš Hájek	JU+IBOT	BOTA	01/08-23/08
Martin Hanáček	MU+JU	GEO	04/07-25/07
Zuzana Chladová	UFA+JU	CLIMA	04/07-19/07
Karel Janko	IAPG+JU	ZOO	01/08-23/08
Jan Kavan	JU	HYDRO	01/07-31/08
Kateřina Kopalová	UK+JU+IBOT	HYDRO	21/07-02/08
Jana Kvíderová	IBOT+JU	MICRO	18/07-02/08
Kamil Láska	MU+JU	CLIMA	04/07-19/07
Daniel Nývlt	MU+CGS+JU+UK	GEO	11/07-25/07
Jan Pačes	IMG	ZOO	08/08-23/08
Václav Pavel	UPOL+JU	ZOO	01/08-16/08
Eveline Pinseel	UA	HYDRO	18/07-02/08
Ekaterina Pushkareva	JU	MICRO	18/07-16/08
Zdeněk Stachoň	MU	GEO	04/07-19/07
Otakar Strunecký	JU+IBOT	MICRO	01/07-19/07
Tomáš Tyml	JU+PARU	ZOO	01/08-31/08
Jakub Žárský	JU+IBOT	MICRO	11/07-02/08

Abbreviations:
Affiliations: CGS – Czech Geological Survey, Brno (CZ); IAPG – Institute of Animal Physiology and Genetics AS CR, Liběchov (CZ); IBOT – Institute of Botany AS CR, Třeboň (CZ); IMG – Institute of Molecular Genetics AS CR, Prague (CZ); IRSM – Institute of Rock Structure and Mechanics AS CR, Prague (CZ); ISB – Institute of Soil Biology AS CR, České Budějovice (CZ); JU – University of South Bohemia, České Budějovice (CZ); MU – Masaryk University, Brno (CZ); PARU – Institute of Parasitology AS CR, České Budějovice (CZ); UA –University of Antwerp, Antwerpen (BE); UFA – Institute of Atmospheric Physics AS CR, Prague (CZ); UK – Charles University, Prague (CZ); UPOL – Palacký University, Olomouc (CZ).
Groups: BOTA - botany/plant physiology; CLIMA - climatology/glaciology; GEO - geology/geomorphology; HYDRO - hydrology/limnology; MICRO - microbiology/phycology; ZOO - zoology/parasitology.

3. Field work progress reports

3.1. Geology and Geomorphology

3.1.1. Fluvial and slope processes monitoring in Petuniabukta

Jan Blahůt, Jan Kavan & Alex Bernardová

After the start of Bertilbreen outwash plain monitoring and scanning of the debris flow cone in 2012, this season we continued with work on these two localities. We also applied a simple vegetation mapping to assess the (in)stability of monitored debris flow cone (Fig. 3.1.1.).

After LiDAR campaign in 2012 the same area has been measured again on August 11th 2013. We will be able to compare DEMs from two consecutive years and evaluate the magnitude of change and identify most active parts of outwash plain. A significant change in morphology of the outwash plain is awaited in the south-western area where a death ice core has been completely washed out during July 2013. The area of the outwash plain has been remodelled almost completely as well. Methodology and detailed description of study area could be found in previous report from 2012.

Fig. 3.1.1. Laser scanning on Bertilbreen outwash plain.

A second part of LiDAR investigation was focused on monitoring debris flow cone located in the vicinity of Czech research station in Petuniabukta (Fig.3.1.2.). The whole area was scanned in 2012 and DEM produced. This has been repeated this season as well. Apart that, a time-lapse camera has been installed to monitor the fluvial and slope movement activity in 2012. We were therefore able to capture the abrupt slush-flow occurred on June 4th 2013 at approximately 2:00 o´clock morning. The amount of material transported by such event will be estimated based on the DEM difference of two LiDAR campaigns. The whole area has been also photographed with help of remote-control helicopter mini-camera. A vegetation mapping has been carried out on 4 cross sections of the flow-cone to gain additional information about stability/instability of the terrain and probability and frequency of such events. Each species of plant grow on surface more or less affected by the slope movements. On that basis we are able to estimate the most probable tracks of regular slash-flows. First „colonizer" of disturbed surfaces is usually *Saxifraga oppositifolia* whereas i.e. *Salix polaris* usually grows on well- established stabilized surface (Fig. 3.1.3.).

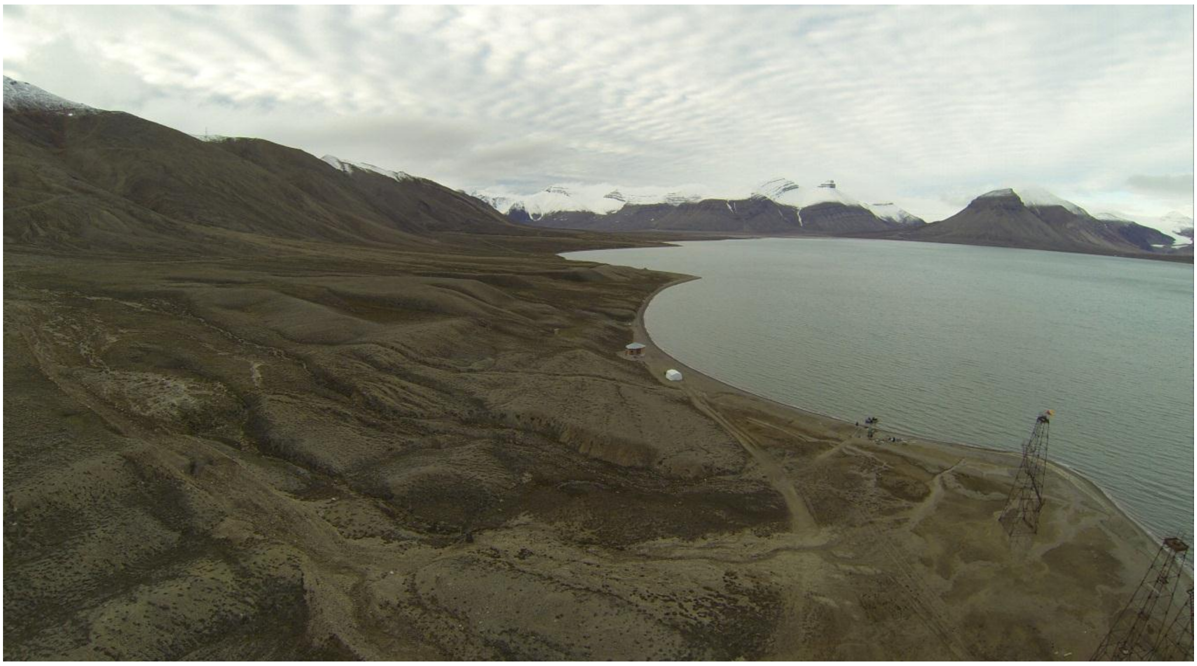

Fig. 3.1.2. Aerial view of the debris flow cone recorded by the remote control helicopter camera.

Fig. 3.1.3. Vegetation mapping on the study area.

3.1.2. Fossil coarse-grained glaciomarginal delta in front of Bertilbreen

Martin Hanáček & Daniel Nývlt

The object of our research has been the deltaic body exposed due to fluvial erosion in the front of Bertilbreen. Sedimentary facies, as well as pebble clasts' petrological composition and shapes have been studied on sections located in proximal and distal part of the delta. Well-preserved bivalves shells have been determined in fossiliferous layers. Delta body is located approx. 50 m above the present sea level.

The proximal part of the delta is made of ~6 m thick gravel foreset and covered by a well-defined topset made of horizontal gravel beds (Fig. 3.1.4.). Foreset dips towards SE, i.e. the recent Mimerbukta Bay. Subglacial till rests on basement below the distal part. Till clasts bear traces of active subglacial transport (subangular and subrounded clasts prevail, high share of striated clasts). Subglacial tills are covered by ?supraglacial tills and other diamictons, their origin will be studied in future. Deltaic foreset consisting of gravel and fine sand layer rests on glacigennic sediments. Shells of *Mya truncata, Macoma calcarea* and *Hiatella arctica* bivalves have been found in sandy facies (Fig. 3.1.5.).

Fig. 3.1.4. Proximal part foreset and topset of a fossil coarse-grained glaciomarginal delta in the Bertilbreen forefield.

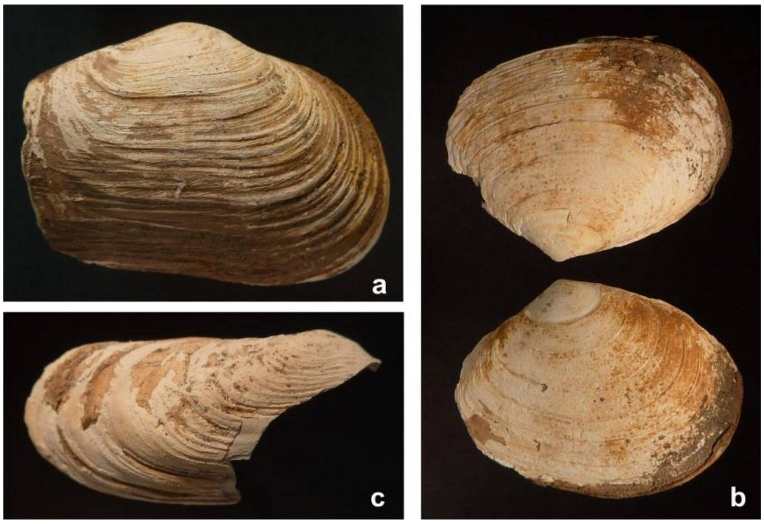

Fig. 3.1.5. Bivalves shells origination of deltaic sand layers. (a) *Mya truncata*, (b) *Macoma calcarea*, (c) *Hiatella arctica*.

Delta origin took place during the maximum highstand during the glacier decay after the Last Glacial Maximum. Delta progradated from Bertilbreen valley towards the Mimerbukta Bay. For the next season we plan to continue with this research in this direction:

- facies and petrological analyses to clarify the genesis of indetermined diamictons
- species composition, burial nature and preservation of mollusc shells to reconstruct the conditions at the sea floor during the deposition of fine-grained layers
- ground penetrating radar survey to reconstruct the delta geometry and its relation to the basement morphology.

3.1.3. Esker in Hørbyebreen proglacial zone

Martin Hanáček & Daniel Nývlt

Our research of Hørbyebreen proglacial zone has been complemented with the study of a large esker extending from the glacier front to the Little Ice Age (LIA) frontal moraine in 2013 season. Esker sedimentary facies and architecture have been studied on large outcrops near the Hørbyebreen front (Fig. 3.1.6.). They are represented mostly by large channel gravel infills. One or two sedimentary logs and main facies have been described and interpreted in each channel infill. Photo-documentation allowed sedimentary architectures reconstruction. Clast petrology and shapes analyses have been undertaken in the most common facies. Intermediate and distal esker parts are planned for the research in next seasons. The aim of the study is to reconstruct depositional processes during esker formation, which might bring further details on the last phase of the ablation zone of the Hørbyebreen glacier its the LIA culmination.

Fig. 3.1.6. Esker sediments in the Hørbyebreen proglacial zone.

3.1.4. Sedimentary petrology of glacial sediments e

Martin Hanáček & Daniel Nývlt

We study petrology and shapes of cobbles and pebbles of different genetic types of glacial sediments since 2011. The area of concern includes recent proglacial zones of Hørbyebreen and Bertilbreen glaciers. Our past findings have been complemented by clast petrology of an esker in front of Hørbyebreen and of a fossil glaciomarginal delta in front of Bertilbreen. Existing results allowed introduction of a new method applied to the reconstruction of clasts transport history within the glacial system. Our approach is based on the comparison of the share of very angular and angular clast (RA index) with the share of striated clasts. The use of these parameters allowed for a distinct discrimination of glaciofluvial sediments and subglacial tills. The hitherto used parameters (covariant plot of RA versus C_{40} indices) do not allowed differentiating them. Covariant plot of striation versus RA index could also be used for identification of sedimentary sources for moraine mound complexes, in which material originated from subglacial tills and glaciofluvial sediments are present in changeable amounts (Fig. 3.1.7.).

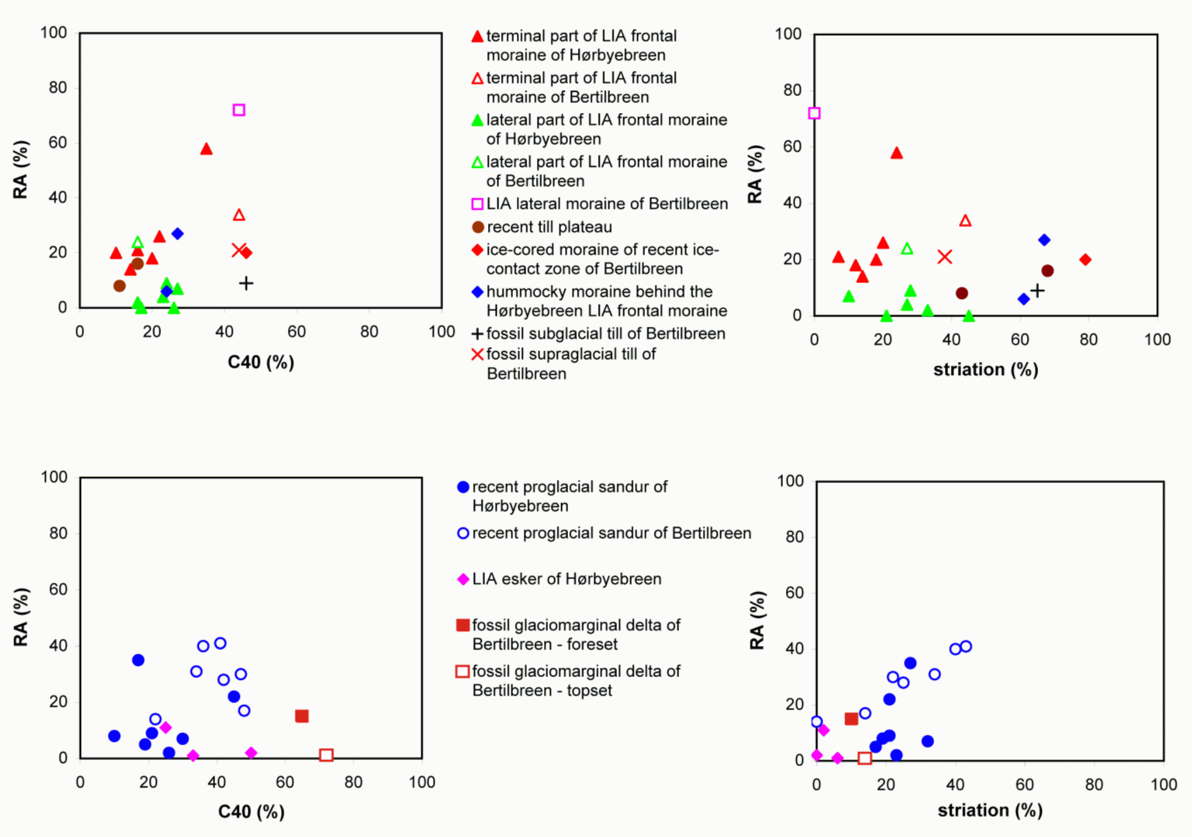

Fig 3.1.7. Covariant plots of C_{40} versus RA and striation versus RA for Old Red sandstone clasts originating from diverse glacial environments of Hørbyebreen and Bertilbreen glaciers.

3.2. Climatology and Glaciology

3.2.1. Meteorology and climatology

Kamil Láska & Zuzana Chladová

The meteorological measurements and observations were performed in the coastal ice-free zone of Petuniabukta, northern branch of Billefjorden in July–August 2013. Nine automatic weather stations (hereafter AWS) were operated along the north-western and eastern coast of Petuniabukta (Fig. 3.2.1.) in the following locations:

- AWS1 – old marine terrace at an altitude of 15 m a.s.l. (operated from 2008)
- AWS2 – old marine terrace at 25 m a.s.l. (operated from 2008)
- AWS3 – foreland of Hørbye Glacier at 67 m a.s.l (operated from 2008)
- AWS4 – mountain ridge of Mumien Peak at 475 m a.s.l. (operated from 2008)
- AWS5 – wet hummock tundra at 8 m a.s.l. (operated from 2009)
- AWS6 – top of Pyramiden Peak at 935 m a.s.l. (operated from 2009)
- AWS7 – Bertil Glacier at 464 m a.s.l. (operated from 2011)
- AWS8 – top of Mumien Peak at 770 m a.s.l. (operated from July 2013)
- AWS9 – foreland of Ragnar Glacier at 92 m a.s.l. (operated from July to August 2013)

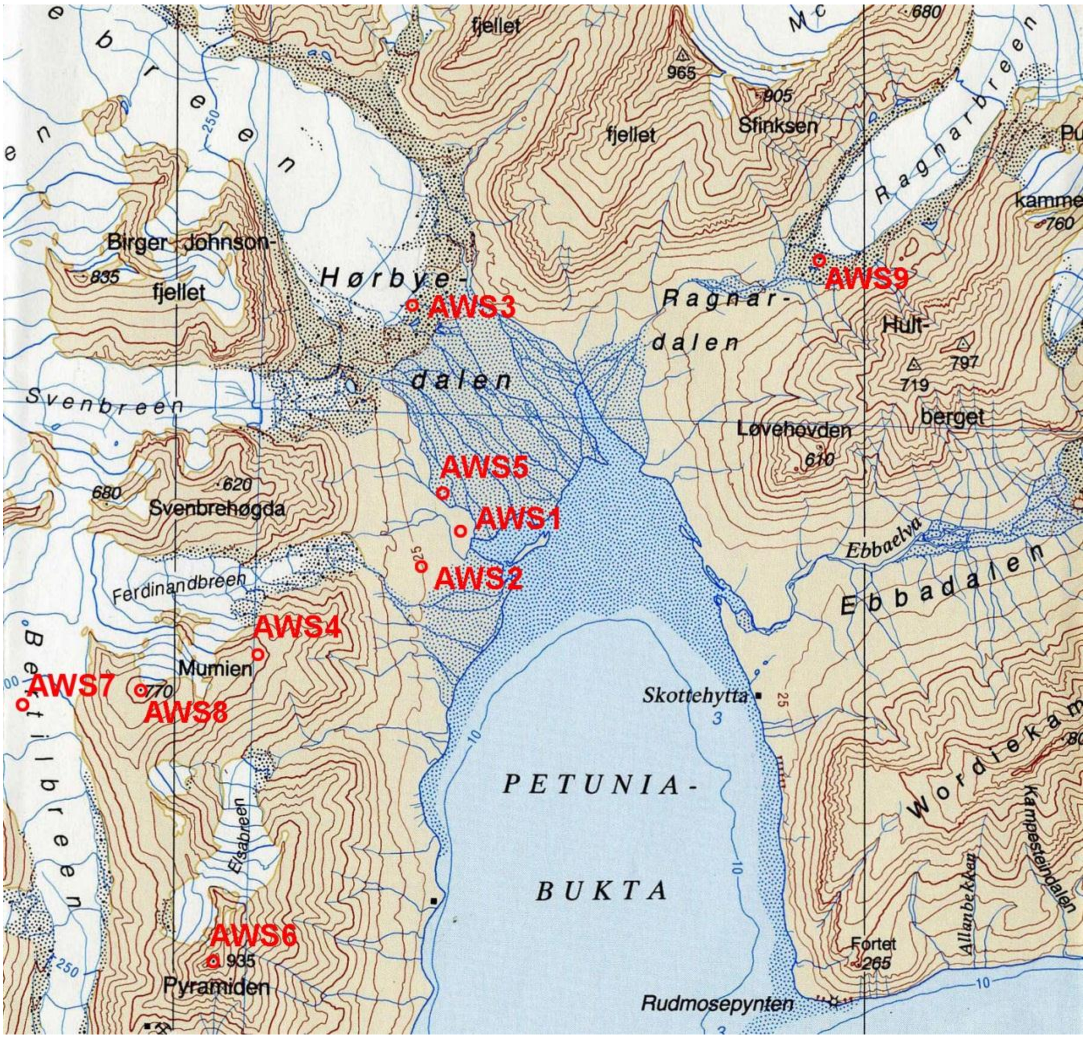

Fig. 3.2.1 Location of the automatic weather stations (AWS) in the vicinity of Petuniabukta (Billefjorden, Spitsbergen) in July–August 2013.

The main objectives of summer field campaign and research activities in Petuniabukta were:

- Measurement of surface energy balance and microclimate of the tundra vegetation
- Monitoring of surface wind characteristics and local phenomena
- Observation of summer weather conditions and their evaluation in the context of large-scale atmospheric circulation over Spitsbergen
- Measurement of small particles (0.02–1 μm) at the selected biotopes
- Maintenance and calibration of the selected meteorological instruments (Fig. 3.2.2.)

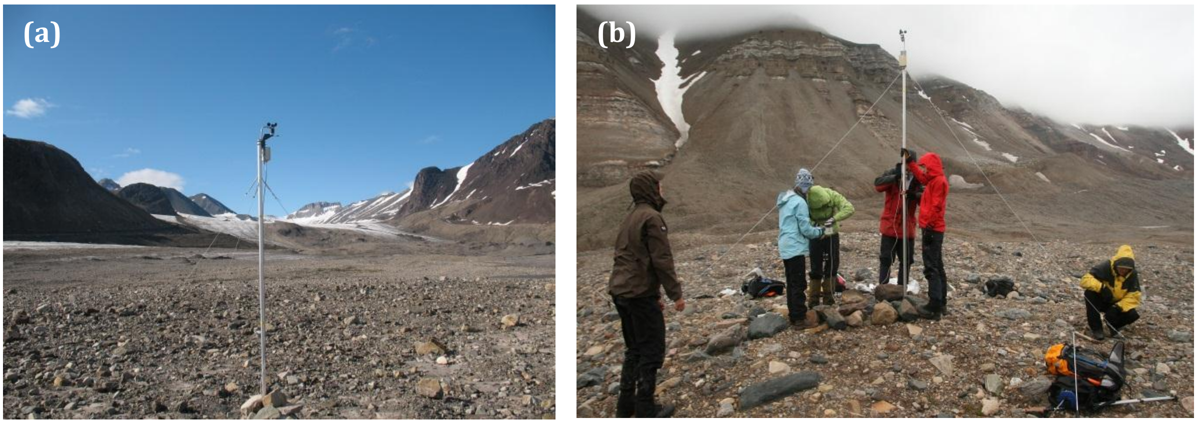

Fig. 3.2.2. Automatic weather stations (AWS) in the vicinity of Petuniabukta **(a)** AWS3 at forelands of Hørbye Glacier, **(b)** AWS9 at Ragnar Glacier.

Short-term study of changes in the microclimate conditions and permafrost active layer properties has been undertaken at the permanent tundra vegetation plot situated on the western coast of Petuniabukta. The records were obtained from automatic micrometeorological station equipped with high precise instruments, which may allow estimation of the surface energy balance and individual fluxes between ground surface and atmospheric boundary layer. During the summer season, incoming and net-radiation showed large fluctuations, primarily caused by variation of cloudiness and cloud types.

Surface wind field experiment was carried out in the vicinity of Petuniabukta in the period July 7–25, 2013. Calculation of wind characteristics was based on measurements of four automatic weather stations located between coastal zone, glaciers and mountain ridges. Inter-daily fluctuations in the surface wind pattern were strongly affected by local topography. We also point at the problem of katabatic winds occurred at the foreland of Hørbye and Ragnar glaciers. A comparison of surface and geostrophic winds were performed in order to assess a role of temperature stratification and large-scale circulation over Spitsbergen area.

In addition to these activities, we carried out maintenance, calibration and replacement of the measuring instruments at all AWS. At the same time, data downloading and quality control of the individual meteorological parameters was performed before further data processing. In August 2013, micrometeorological station together with the AWS9 was winterized. High sensitivity instruments were dismounted and transported to the Czech Republic (Masaryk University, Brno) for calibration and technical service.

In the study period, the atmospheric circulation and pressure pattern changed three times. Between July 6 and 11, 2013, the cyclone moved from Iceland north-eastward over the Svalbard archipelago and then over the Franz Josef Land at the 850 hPa geopotential height. This resulted in prevailing cloudy weather conditions in the region of Spitsbergen and

Petuniabukta, with the cloudiness of 6–8 oktas, and presence of typical cloud types: *stratus nebulosus opacus*, *altostratus* and *altocumulus* (Fig. 3.2.3.). During the second period (July 12–14, 2013), the anticyclonic type of circulation started to prevail. The *cirrus*, *cirrostratus*, *altocumulus lenticularis* and *cumulus humilis* and *cumulus mediocris* clouds occurred in the air masses flowed over Spitsbergen. Moreover, halo phenomena and cloud irisation were observed in Petuniabukta within this situation. In the third period from July 15 to 17, 2013, the cyclonic type of circulation prevailed. The cyclone over North Atlantic disappeared and the cyclone over Novaya Zemlya moved north-westward over the North Pole. The presence of cloud type as *stratus* and *stratocumulus* was observed at Petuniabukta in these days (Table 3.2.1. and Fig. 3.2.4).

Fig. 3.2.3. Three main types of high- and low-level clouds (*cirrus*, *cirrocumulus and orographic stratus*) occurring at Petuniabukta on July 12, 2013.

Tab. 3.2.1. Characteristics of daily mean temperature (AT avg), daily minimum (AT min) and maximum temperature (AT max), average wind speed (VS avg) and maximum gust (VS max), cloudiness (N) and cloud types at low (C_L), middle (C_M) and high level (C_H) at Petuniabukta in the period July 5–19, 2013.

Day	**AT** [°C]			**VS** [m/s]		**N** [0–8]	**Cloud type**		
	avg	min	max	avg	max		C_L	C_M	C_H
5.7.	6.4	5.6	9.5	1.9	3.6	7.7	St	.	.
6.7.	8.7	6.9	11.5	1.9	4.4	7.6	St	.	.
7.7.	8.9	6.7	11.4	2.1	4.6	7.9	St	.	.
8.7.	8.8	6.9	11.7	2.6	4.6	6.9	St	Ac	.
9.7.	7.0	5.5	8.0	2.6	4.5	8.0	St	.	.
10.7.	4.5	3.8	5.4	5.2	10.2	7.7	St	Ac	.
11.7.	5.1	3.8	6.4	6.5	10.2	7.4	Sc/St	As	Ci
12.7.	6.6	4.4	8.4	4.9	6.5	5.7	Sc	Ac/As	Ci
13.7.	8.8	6.1	10.7	4.4	6.4	2.8	Cu/Sc	As	Ci/Cs
14.7.	8.5	5.0	10.7	5.6	8.4	3.3	Sc	Ac	Ci
15.7.	4.4	3.7	5.1	6.0	9.8	7.9	St	Ac	.
16.7.	4.9	3.8	6.4	4.7	7.0	6.7	St	Ac/As	.
17.7.	6.9	4.3	9.0	2.3	4.5	5.1	St	Ac	Ci
18.7.	10.2	7.4	12.2	2.3	4.2	2.9	Cu	Ac	Ci
19.7.	10.6	6.2	13.9	3.2	6.4	5.9	St	Ac	.

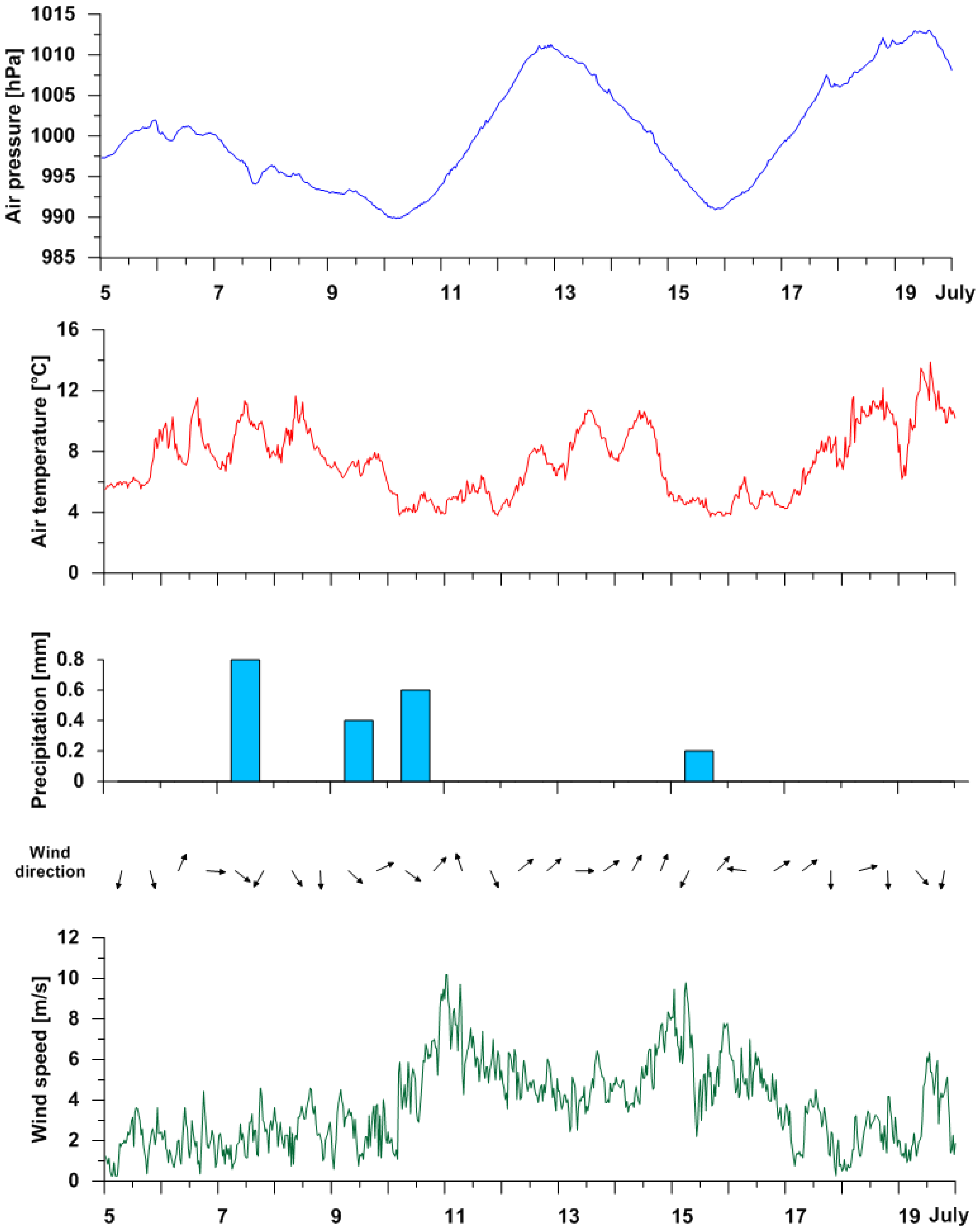

Fig. 3.2.4. Diurnal variation of air pressure, 2-m air temperature, precipitation, 6-m wind direction and wind speed recorded at Petuniabukta in the period July 5–19, 2013.

Ultrafine particle emissions and their spatiotemporal variation were studied at Petuniabukta in July 2013. The amount of small particles (0.02–1 μm) was registered by P-track instrument near the Czech polar station and other sites of Petuniabukta. Fig. 3.2.5. shows the highest amount of these particles during the clear sky conditions on July 13. In another experiment, the particles were measured above different types of ground surface:

coastal zone, mountain area, wet hummock tundra, and glaciers. Furthermore, we compared the relative amount of ultrafine particles between Petuniabukta and Longyerbyen, which is more exposed by emissions from the local sources of the pollution.

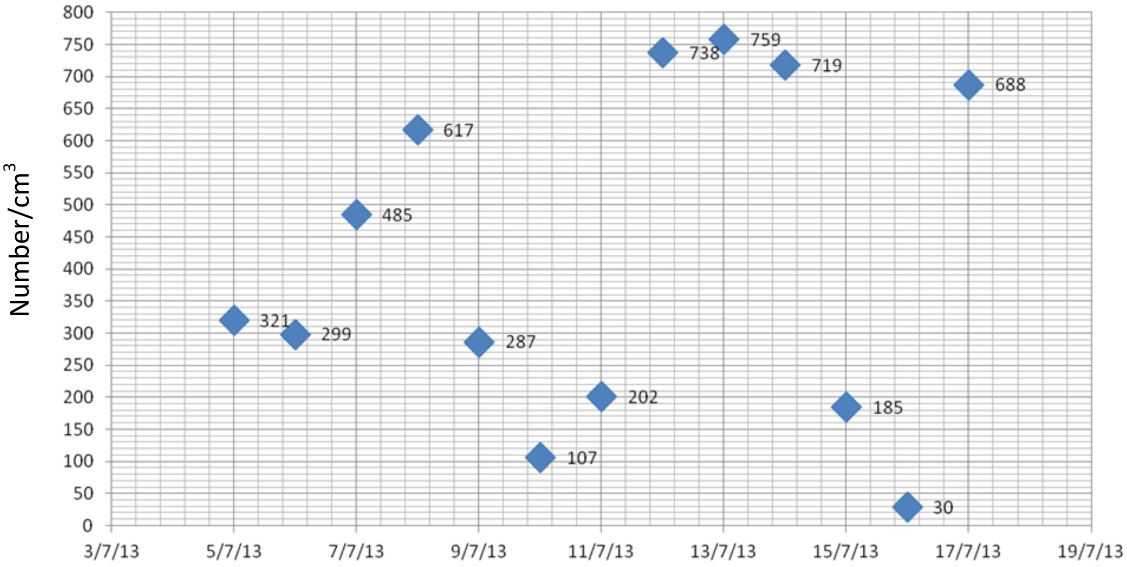

Fig. 3.2.5. Number of ultrafine particles (0.02–1 μm) recorded near the Czech polar station (Petuniabukta, Billefjorden) in the period July 5–19, 2013.

3.3. Hydrology and Limnology

3.3.1. Hydrological monitoring in Petuniabukta

Jan Kavan

Automatic monitoring system has been set up in 2011 on 4 experimental water basins and is now further widening. 3 other sensors were added in 2012 – these were manually calibrated during the 2013 season with use of Flowtracker acoustic current meter. All sensors were working after its defrost usually in the middle of June. Monitoring on Bertilbreen river is used for study of fluvial dynamics and glacier mass balance.

Beside the 7 sensors from 2011 and 2012 seasons a new one has been set up on Mimerdalen lake 1 (78.6245°N, 15.9808°E, Fig. 3.3.1.). The common project (Adam Mickiewicz University in Poznan - Jakub Malecki) on Svenbreen river (78.7276°N, 16.3995°E) continues. Manual discharge measurements and automatic water level observations will be used for assessing glacier meltwater runoff in the complex Sven glacier mass balance study.

All these are part of long-term hydrological monitoring system of selected rivers in Petuniabukta area. This should enable us to observe changes in hydrological and thermal regime related to climate change and consequent retreat of glacier in the area.

Fig. 3.3.1. Mimerdalen lake 1 – new water level sensor has been installed to asses highly variable hydrological regime of the lake; it was estimated that the water level decreases by almost 1 meter during the summer season.

3.3.2. Snow and sea ice monitoring system

Jan Kavan

The snow monitoring system has been established in 2012 as a first try to monitor the snow conditions in Petuniabukta. The time-lapse cameras proven to be a good tool for such monitoring even with some troubles of capturing images during the lowest temperatures (typically below – 20°C the chip does not record the image correctly). However the cameras are working well during spring that is the most important part of year regarding snow accumulation and further start of melting season.

It is obvious that the characteristics of snow cover are crucial for most of the environmental processes taking place during summer season. These characteristics influence soil and permafrost properties, hydrological regime but also all the terrestrial biota.

The images were processed and evaluated (Fig. 3.2.2.). On this basis it was decided to perform some slight changes in installation design – the ablation stakes that were more than 50 metres from the camera were not possible to use for snow depth estimation. Position of the camera has been changed and moved directly to the main AWS, where also set of 10 ablation stakes were established. The camera intended to be used for sea ice monitoring has unfortunately been destroyed during the winter with no images recovered. On the other hand, camera used for slope processes monitoring on the debris flow cone quite well captured also the snow depth evolution during winter and especially during spring melting season. In general, no more than 30cm of snow has been recorded on all 3 cameras during winter 2012/2013 which seems to be quite low state of snow depth.

Fig. 3.3.2. Snow cover on June 4th 2013 on the debris flow cone locality – just after the slash-flow occurred.

3.3.3. Reconstruction of Holocene environmental conditions from lake sediment

Daniel Nývlt, Kateřina Kopalová, Jan Kavan, Eveline Pinseel, Matěj Roman & Daniel Vondrák

This season a special attention has been paid on the Garmaksla locality. During last season this locality has been proven to have relatively thick sediment layer in the central part of the lake basin. Therefore a field campaign focused on extracting sediment cores has been carried out in July 2013 (27/07/2013). Three sediment cores have been taken with help of gravity corer - 79, 72 and 66cm long. The cores have been subsampled directly on the site – each were cut in 1cm interval and stored in plastic sacks (Fig. 3.3.3.).

Sediment cores will be used for basic geological/sedimentological analyses and this will be done by Matěj Roman and Daniel Nývlt. Further proxies, such as magnetic susceptibility, organic and inorganic carbon, sulphur and basic elements content, together with grain-size will be analysed in the laboratories in Czechia to complement the ascertained ecosystem changes. Second part consists of analyses of zooplankton species diversity (*Micropsetra radialis*, *Orthocladius trigonolabis* etc.) - Daniel Vondrák; and especially the third part focused on diatom assemblages – Kateřina Kopalová, Eveline Pinseel. General hydrological conditions of the lake ecosystem with thermal regime and Holocene landscape evolution will be described as well – Jan Kavan, Daniel Nývlt.

Fig. 3.3.3. Sediment core from Garmaksla lake – 27/07/2013 photo: Daniel Vondrák.

Diatoms (Bacillariophyta) are one of the most abundant algal groups in polar ecosystems and they proved to be very useful indicators of environmental and climatic changes in polar region. During the 2013 summer (but also last polar summers 2011 and 2012) set of lakes and terrestrial ecosystems in the vicinity of Petuniabukta (Central Spitsbergen) were sampled. Both physico-chemical parameters and variety of biological markers were studied.

Freshwater and terrestrial diatom composition will be analysed in the samples, using light microscopy and, when appropriate, scanning electron microscopy techniques. Transfer functions for the significant environmental parameters will be developed on the basis of specific diatom composition (Fig. 3.3.4.).

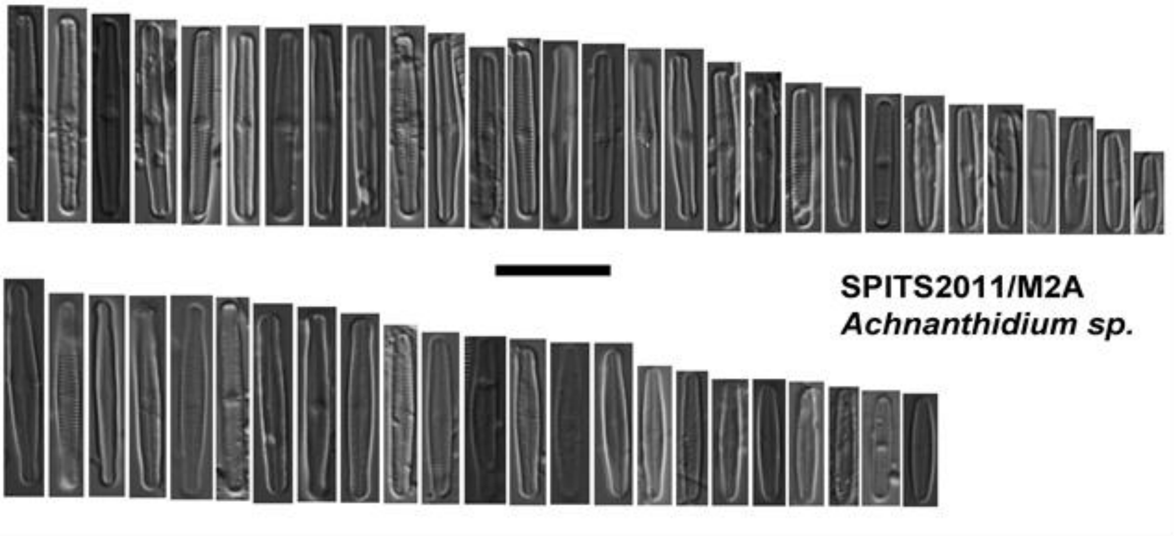

Fig. 3.3.4. New species found in recent samples - previously belonging to *Achnanthidium minutissimum* but needs to be described as a separate species (probably even two more new *Achnanthidium* species found) – photo: Eveline Pinseel.

3.4. Microbiology and Phycology

3.4.1. Simulation of climatic change in modified OTCs in wet hummock tundra

Josef Elster, Jana Kvíderová, Tomáš Hájek, Kamil Láska & Miloslav Šimek

In 2013 we completed the study of the simulation of climatic change in modified OTCs in wet hummock tundra that had been performed since 2009. The studies of effect of simulated warming were focused on (i) photosynthetic and nitrogenase activity in a cyanobacteria *Nostoc* and on (ii) cellulose decomposition rate as a measure nutrient mineralization potential.

OTC rather prolonged than accelerated the vegetative season as compared with CCS. The maximum prolongation was 30 days in hummock bases (2012) and 17 days in tops (2011). OTC increased mean temperature of the vegetation season in hummock tops by <1 °C in 2010–11 and by 2.7 °C in 2012 (covered OTC) while there was no increase in much wetter hummock bases. Analogously, annual maxima greatly increased in hummock tops but little, if ever, in bases. OTC affected soil VWC only slightly (Table 3.4.1.).

Table 3.4.1. The microclimatic parameters in OTCs and CCSs during the experiment for each vegetative season. Start date – temperature remained above 0 °C for whole day; End date – VWC dropped to 0 for the first time (the water froze).

	Open Top Chambers (OTC)				Control Cage-like Struture (CCS)				Difference OTC–CCS	
	Hummock top		Hummock base		Hummock top		Hummock base		Hummock top	Hummock base
	mean	sd	mean	sd	mean	sd	mean	sd		
Vegetative season 2009										
End date	**15 Sep**	1	**06 Oct**	48	**15 Sep**	0	**30 Sep**	1	**0**	**6**
Vegetative season 2010										
Start date	**09 Jun**	7	**16 Jun**	4	**12 Jun**	4	**17 Jun**	2	**-3**	**-2**
End date	**25 Sep**	1	**22 Oct**	4	**13 Sep**	0	**14 Oct**	2	**12**	**8**
Duration (days)	**108**	6.6	**128**	1.2	**93**	4.2	**119**	4.2	**15**	**9**
T mean (°C)	**7.5**	0.4	**3.7**	0.2	**6.7**	0.3	**3.6**	0.1	**0.8**	**0.1**
T max (°C)	**28.2**	1.5	**12.7**	1.5	**20.6**	4.0	**13.3**	0.4	**7.6**	**-0.6**
RWC mean (m3/m3)	**0.06**	0.01	**0.35**	0.02	**0.06**	0.01	**0.35**	0.05	**0.00**	**0.00**
Vegetative season 2011										
Start date	**19 Jun**	2	**22 Jun**	2	**21 Jun**	0	**22 Jun**	1	**-2**	**1**
End date	**05 Oct**	1	**18 Oct**	13	**18 Sep**	0	**06 Oct**	1	**17**	**12**
Duration (days)	**108**	2.6	**118**	12.5	**89**	0.0	**107**	2.1	**19**	**11**
T mean (°C)	**7.7**	0.4	**5.2**	1.7	**6.8**	1.1	**5.2**	0.8	**0.9**	**0.0**
T max (°C)	**27.1**	1.3	**13.5**	3.1	**19.5**	5.2	**11.3**	1.0	**7.6**	**2.2**
RWC mean (m3/m3)	**0.08**	0.01	**0.30**	0.01	**0.06**	0.02	**0.3**	0.1	**0.02**	**-0.01**
Vegetative season 2012										
Start date	**20 Jun**	4	**20 Jun**	3	**19 Jun**	1	**19 Jun**	4	**1**	**1**
End date	**26 Sep**	1	**06 Nov**	7	**20 Sep**	0	**07 Oct**	0	**6**	**30**
Duration (days)	**98**	4.9	**139**	6	**93**	1.4	**110**	4.2	**5**	**29**
T mean (°C)	**9.1**	0.4	**3.9**	0.4	**6.4**	0.4	**4.2**	0.1	**2.7**	**-0.3**
T max (°C)	**28.7**	1.7	**13.1**	2.1	**17.0**	1.9	**11.2**	0.9	**11.8**	**2.0**
RWC mean (m3/m3)	**0.07**	0.01	**0.35**	0.03	**0.07**	0.00	**0.4**	0.1	**-0.01**	**-0.02**
Vegetative season 2013	**(till 5 Aug 2013 only)**									
Start date	**15 Jun**	3	**18 Jun**	3	**15 Jun**	2	**18 Jun**	2	**-1**	**0**
T mean (°C)	**10.9**	1.6	**7.2**	0.2	**9.2**	0.1	**7.1**	0.2	**1.7**	**0.2**
T max (°C)	**29.2**	4.4	**14.1**	2.4	**22.7**	2.9	**15.1**	1.8	**6.6**	**-0.9**
RWC mean (m3/m3)	**0.08**	0.01	**0.35**	0.04	**0.08**	0.00	**0.37**	0.04	**0.00**	**0.00**

As the OTC did not affect microclimatic conditions in hummock bases, the *Nostoc* colonies living there were not influenced by OTC in terms of photosynthetic and nitrogenase activities. Nevertheless, the activities were greatly influenced by varying weather conditions affecting current hydration of the colony since the colonies often desiccate on the soil surface. Surprisingly, photosynthetic and nitrogenase activities usually did not correlate.

There was no effect of OTC on cellulose decomposition rate but it was lower in hummock bases as compared to hummock tops (p=0.02, n=24), probably due to water-saturated and colder conditions in mossy bases.

Open top chambers installed in wet hummock tundra provided small greenhouse warming effect and only on top of hummocks. Although closed OTC considerably increased the temperature in hummock tops and prolonged vegetation season in bases, cautious interpretation of such results is required. Shoot hydration is the most significant environmental factor affecting physiology of poikilohydric *Nostoc* colonies as well as the decomposition potential in hummock tundra.

At present, there are other OTCs located on the top of the Mumien Peak, near the main weather station and in front of Hørbyebreen glacier on deglaciated moraine used for studies on warming effect (OTC) on soil microbial and invertebrate communities remain in operation.

3.4.2. Supraglacial life

Jakub Žárský

In the period from 11 July to 2 August 2013 a field campaign was conducted in the area of Petunia bay (central Spitsbergen, Svalbard archipelago). The there were two goals of the mission: i) survey focused on finding optimal localities for fieldwork with students participating on the Course of Polar Ecology and to establish a concept of a lecture (delimitating field and analytical methods and fieldwork safety), ii) survey of glaciers adjacent to Petuniabukta with respect to supraglacial life.

On the Hørbye glacier, Ferdinand glacier, Jotun ice cap (Jotunfonna; Fig. 3.4.1.) and Bertil glacier, image data of the surface were collected using standardized photography for estimation of coverage of cryoconite using image analysis (ImageJ 1.43u, script of Irvine-Fynn et al., 2010). We sampled cryoconite in simple altitudinal transects in the central line of the glaciers (eastern slope in the case of Jotun ice cap, Fig. 3.4.2.) and measured basic physical parameters of the melt water (pH, conductivity).

Fig. 3.4.1. Jotun glacier from the northern slope of Garmaksla. See fulmar nesting sites indicated by orange coloration by a lichen *Xanthonema elegans*.

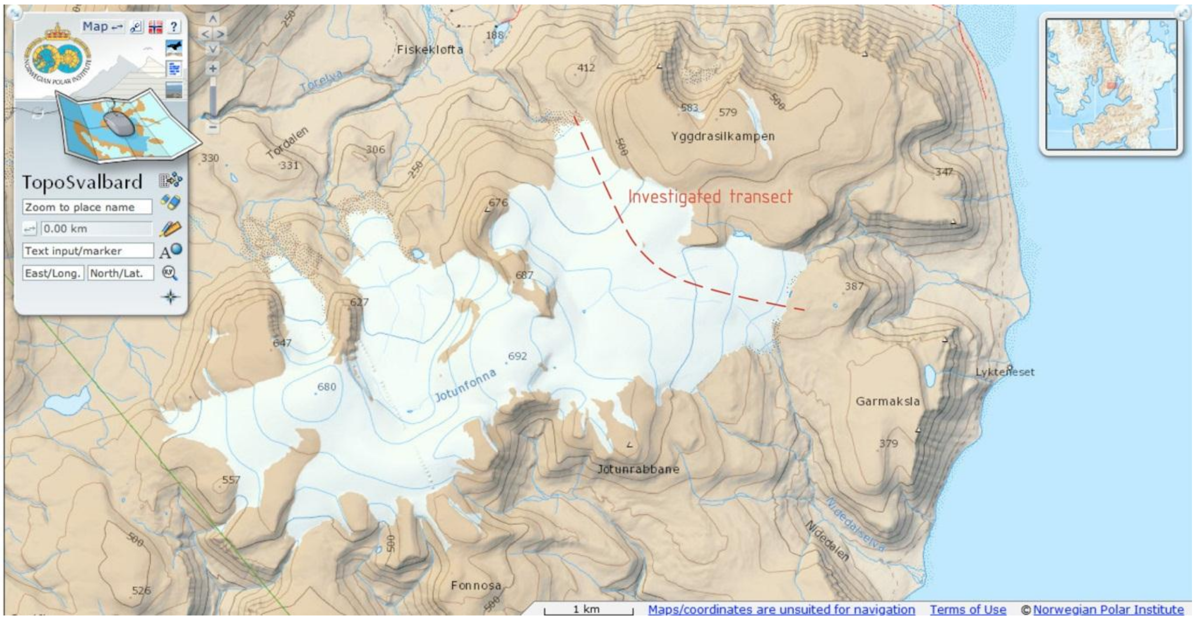

Fig. 3.4.2. Overview map of the Jotun glacier transect. The highest abundance of bryophytes on the glacier surface was in the eastern part of the transect. Map source © Norwegian Polar Institute.

In the case of Hørbyebreen sampling sites were added also to the southern and northern sides of the glacial stream). Samples were kept on ice during the transport from the glacier to the base to avoid a heat shock of the organisms. Unfixed samples were investigated under microscope (Olympus BX-53). Aliquots of samples were then air dried and transported to the laboratory for chemical investigation of the sediment.

The organisms found in the samples didn't exceed the range of species and genera usually reported from cryoconite in Svalbard (from green algae: *Chlamydomonas nivalis*, *Cylindrocystis brebissonii*, *Ancylonema nordenskjoeldi*, in Tardigrada and Rotifera samples were taken for determination by a specialist) with one exception: namely occurrence of "joklamys" (glacial mice), cushions of bryophyte with spherical growth forms in the frontal areas of glaciers (Fig. 3.4.3.).

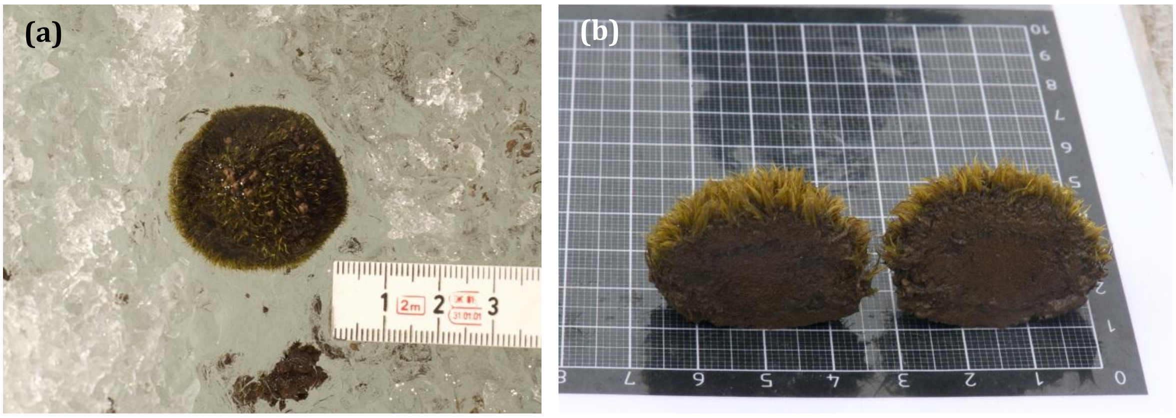

Fig. 3.4.3. Bryophytes of the Jotun glacier. **(a)** Bryophyte *in situ* on the surface of the glacier, **(b)** cross-section of a bryophyte with pronounced concentric layers at the profile.

The bryophytes were previously reported especially from glaciers at Island (Porter et al., 2008) and some reports are also from Svalbard (e.g. Grønfjordbreen, UNIS field reports, A. Hodson, personal communication). We have found the bryophytes in various densities on all investigated glaciers. Most surprising was high density of grown (macroscopically visible) bryophyte colonies on Jotun ice cap, which has no adjacent slopes, which indicate low (or not at all) allochtonous origin of the bryophyte biomass. We also report occurrence of initial stadia of mosses in cryoconite aggregates. These aggregates don't differ in size or morphology from aggregates reported elsewhere when investigated by naked eye. Microscopical investigation however revealed dense net of protonemata/rhizoides and the aggregates are mechanically stabilized. Thus we would like to focus on this phenomenon also in the next season and experimentally test a hypothesis about the effect of bryophytes on cryoconite retention in the frontal area of the glaciers. Data from the season 2013 will be used for the experimental design and published output.

References:

Irvine-Fynn, T.D., Bridge, J.W., Hodson, A.J., 2010. Rapid quantification of cryoconite: granule geometry and in situ supraglacial extents, using examples from Svalbard and Greenland. J. Glaciol. 56, 297–308.

Porter, P.R., Evans, A.J., Hodson, A.J., Lowe, A.T., Crabtree, M.D., 2008. Sediment-moss interactions on a temperate glacier: Falljokull, Iceland. Ann. Glaciol. 48, 25–31.

3.4.3. Diurnal changes in photochemical activity in soil crusts

Ekaterina Pushkareva

In period from July 18 till August 16 I participated in Arctic expedition following polar ecology course organised by Polar Ecology Center. The course took place in Petunia Bay, Svalbard. My aim of this course was to study different types of soil crusts. Within this aim I measured photosynthetic activity of soil crust surface using FluorPen. To prove that photosynthetic organisms are mostly located on surface FluorCom was used. It shows that these organisms penetrate 1-2 cm of soil crust (Fig. 3.4.4.).

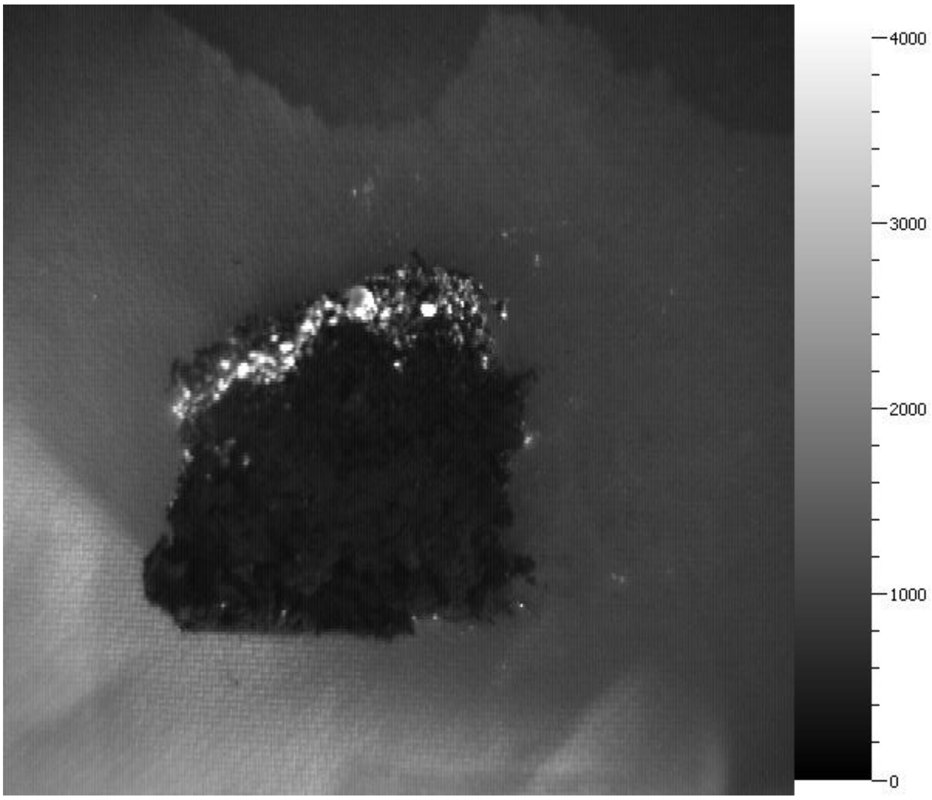

Fig. 3.4.4. Fluorescence image of soil crust showing photosynthetic activity in upper layer.

By the FluorPen I measured diurnal cycle of photosynthetic activity (QY – Quantum Yield) in light conditions and with dark adaptation for three different types of soil crust: algal, cyanobacterial and poor (Fig. 3.4.5.). It is visible that QY in poor soil crust almost doesn't changed in compare with algal and cyanobacterial crusts.

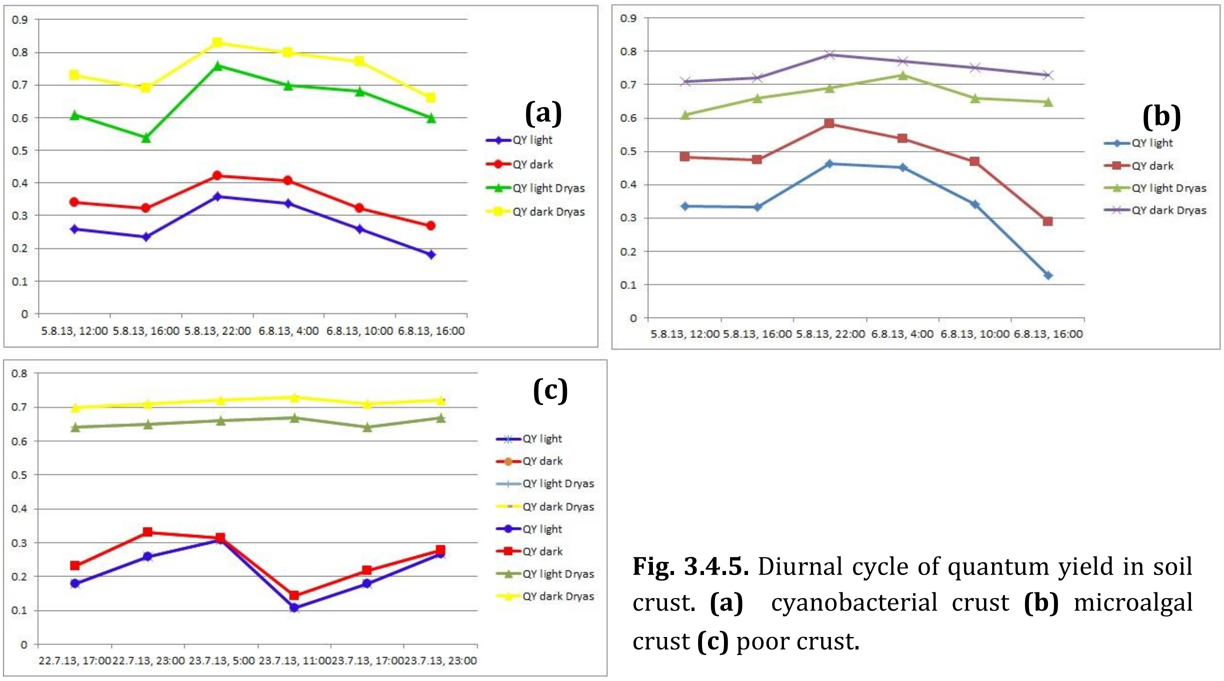

Fig. 3.4.5. Diurnal cycle of quantum yield in soil crust. **(a)** cyanobacterial crust **(b)** microalgal crust **(c)** poor crust.

3.4.4. Photochemical activity at surface and the bottom of microbial mats and *Nostoc* colonies

Jana Kvíderová

Microbial mats are common in all hydro-terrestrial and terrestrial communities in the polar regions. They may be formed by one species or by several prokaryotic/eukaryotic species and could be up to several mm thick. The internal structure of *Nostoc* colonies (Cyanobacteria), also belonging to dominant phototrophic (micro)organisms in the polar regions, may resemble microbial mats as well (Fig. 3.4.6.). Due to light absorption by cells, extracellular matrix and inorganic particles, different irradiance conditions occur at the surface and the bottom of the mat.

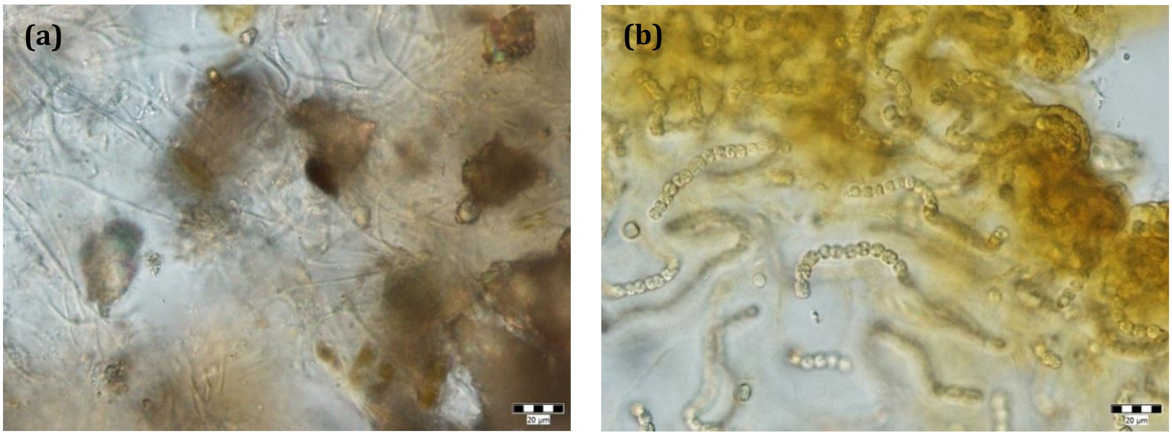

Fig. 3.4.6. Similarity in ultrastructure of microbial mats and the *Nostoc* colonies. **(a)** microbial mat **(b)** *Nostoc* colony.

The photochemical activity of the microbial mats and *Nostoc* colonies collected near the station was evaluated using fluorescence imaging camera FluorCam and the NPQ protocol was applied. Several fluorescence parameters describing the photochemical performance were calculated: the maximum quantum yield (F_V/F_M), actual quantum yield (QY), non-photochemical quenching (NPQ) and photochemical quenching (qP).

Different response of mat surface and bottom to incoming light were observed in both high and low light. The decreased values of F_V/F_M and QY of mat surface might indicate photoinhibition. However, lower values of NPQ and increased values of qP are typical for photoacclimated samples. The actinic light of 150 µmol m^{-2} s^{-1} was probably too high for bottom layers and induced faster activation of photoacclimation mechanisms. At the surface, the microorganisms were acclimated to increased irradiances, even higher than that of actinic light used (Table 3.4.2.).

Contrary to microbial mat, *Nostoc* colonies, the differences between the exposed and shaded sides of the colonies were minimal. The irradiance seems to be more important factor affecting whole colony. The *Nostoc* colonies were photoinhibited during high light treatment as seen from decreased qP and increased NPQ (Table 3.4.2.).

Table 3.4.2. The photochemical parameters of the microbial mat and the *Nostoc* colonies at high and low light conditions (n = 5 in each case). L, S, LS - statistically significant differences ($P<0.05$) for light treatment (L), structure (S) and combination of light treatment and structure (LS; two-way ANOVA).

	Microbial mat					***Nostoc***				
	High light		Low light			High light		Low light		
	Bottom	Surface	Bottom	Surface		Bottom	Surface	Bottom	Surface	
F_V/F_M										
Mean	**0.474**	**0.310**	**0.454**	**0.346**		**0.520**	**0.464**	**0.450**	**0.412**	L
Min	0.420	0.270	0.430	0.290	S	0.500	0.400	0.370	0.320	S
Max	0.530	0.370	0.500	0.370		0.550	0.520	0.500	0.490	
s.d.	0.044	0.038	0.028	0.033		0.020	0.051	0.051	0.063	
QY										
Mean	**0.154**	**0.134**	**0.196**	**0.164**	L	**0.226**	**0.246**	**0.272**	**0.248**	
Min	0.130	0.110	0.170	0.150	S	0.220	0.190	0.200	0.210	
Max	0.200	0.160	0.230	0.170		0.240	0.280	0.310	0.290	
s.d.	0.027	0.018	0.022	0.009		0.009	0.034	0.047	0.033	
NPQ										
Mean	**0.298**	**0.150**	**0.252**	**0.206**		**0.162**	**0.140**	**0.100**	**0.112**	L
Min	0.250	0.130	0.170	0.140	S	0.140	0.090	0.080	0.060	
Max	0.350	0.170	0.340	0.240	LS	0.200	0.210	0.140	0.170	
s.d.	0.048	0.016	0.068	0.040		0.024	0.047	0.028	0.041	
qP										
Mean	**0.372**	**0.476**	**0.490**	**0.542**	L	**0.470**	**0.568**	**0.636**	**0.642**	L
Min	0.350	0.440	0.440	0.520	S	0.450	0.500	0.580	0.520	
Max	0.430	0.500	0.530	0.560		0.500	0.660	0.710	0.710	
s.d.	0.033	0.023	0.046	0.015		0.020	0.066	0.053	0.073	

The different response of the microbial mats and *Nostoc* colonies may be caused by their different ultrastructure. The microbial mat is compact and firm, so more light energy is absorbed by its surface layer, resulting in quite different light conditions at the surface and bottom. The *Nostoc* colonies are more translucent than the mats, since they contain large amounts of translucent extracellular matrix, so the light may penetrate even to bottom layers.

Thus, difference in light conditions at surface and bottom of the colony is not so pronounced as in mats.

3.5. Botany and Plant Physiology

3.5.1. Effect of simulated warming on plant cover and decomposition

Tomáš Hájek

We terminated the four-year experiment studying warming effect of open top chambers (OTC) on vegetation and potential decomposition in wet hummock tundra. The warming increased mean growth season temperature in top soil particularly in OTCs (1.5–3.0 °C) but less in wet hummocks bases (0.2–0.8 °C). The warming also postponed the end of growth reason by one to four weeks.

There was striking increase of vascular aboveground biomass inside the OTC and control cages where the vegetation was protected from grazing. As a result, the effect of grazing seemed to overrule the effect of warming in both, hummock tops and bases. Common horsetail *Equisetum arvense* showed the greatest increase in aboveground biomass when protected against geese grazing. In agreement with that, the geese have grazed most of the horsetail biomass within two days after removal of OTCs and control cages in the end of the experiment.

We expected that the warming effect on decomposition potential (a proxy for biomass mineralization rate expressed as cellulose mass loss) will differ between drier elevated hummocks and wet and colder depressions. Although the decomposition potential was greater in hummock than in depressions, there was no warming effect of OTC as compared with control cages.

3.5.2. Ecology of wet hummock tundra

Tomáš Hájek

Hummocks of wet tundra consist entirely of peat with no evidence of having a cryogenic origin. Therefore I asked whether decomposition processes, namely adverse abiotic conditions in hummocks and greater recalcitrance of litter of hummock-forming plants, may explain persistence of elevated peat hummocks as in case of boreal peatlands.

Reciprocal transplant decomposition experiment has been established in wet hummock tundra in 2009. Four litter types were incubated for two and four years in both microhabitats, hummock tops and bases: (i) a moss *Scorpidium cossonii* from wet hummock bases, (ii) mosses from dry hummock tops, (iii) macroscopic colonies of a cyanobacterium *Nostoc* that are common in the wettest microhabitats, and (iv) cellulose as a standard material used in decomposition experiments (Fig. 3.5.1.).

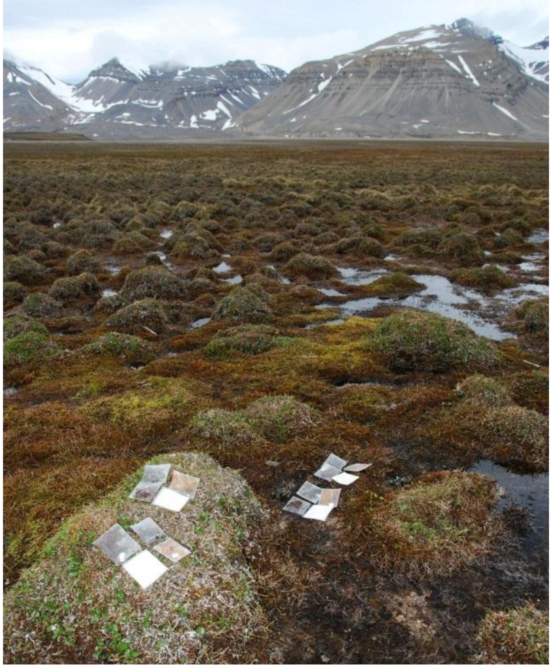

Fig. 3.5.1. Litter bags show their position in hummocks tops and bases, before placed below the surface for two or four years.

Preliminary results indicates that hummocks are more suitable environment for microbial decomposition than the water-saturated depressions and that the hummock-forming mosses are more decomposable than mosses from wet bases, irrespective of incubation position. This is rather weird result but data from the second incubation period will provide more information.

3.5.3. Seed dispersal

Alexandra Bernardová

This season we have continued in the study of seed dispersal possibilities of arctic plants via excrements of reindeer (*Rangifer tarandus var. Spitzbergensis).* The feces of reindeer were collected into the plastic bags. In the laboratory in Ceske Budejovice the feces were diluted in water, sieved through the mesh 0.25mm and the seeds were picked up, counted and the viability of seed was estimated. Animals could serve as seed distributors via their feces and thus enhancing the colonisation of deglaciated, disturbed or newly emerged areas. According the preliminary results, it seems, that high percent of seeds distributed by reindeers is viable (Fig. 3.5.2.).

The most frequent were seeds of *Saxifraga oppositifolia, Silene furcata* and *Saxifraga aizoides*. Interesting is the number of *Cassiope tetragona* seeds, as it is supposed, that the reindeers do not eat *Cassiope* at all.

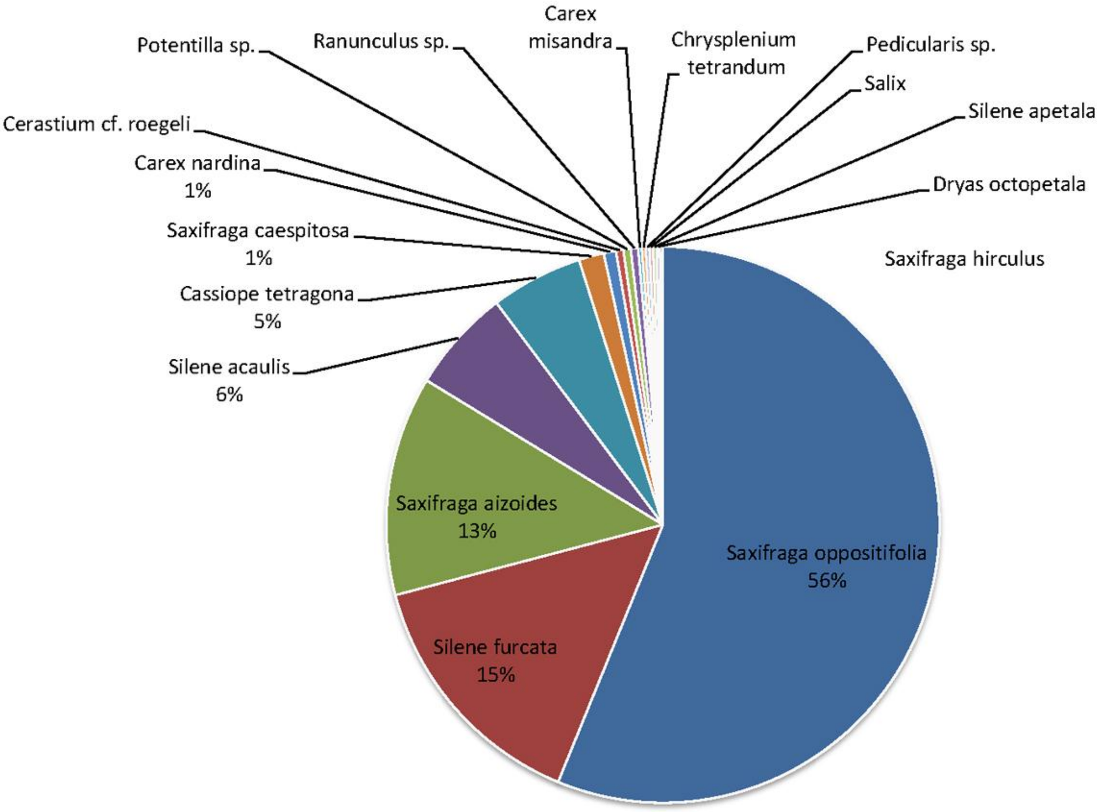

Fig. 3.5.2. The proportion of viable seeds found in analysed samples.

3.5.4. Pollen traps

Alexandra Bernardová

In the area of Petuniabukta, two pollen monitoring traps (http://www.pollentrapping.net/) were installed (Fig. 3.5.3.). The first was installed in the tundra on the terrace in the vicinity of AWS1 (Fig. 3.5.4.) and the second one at the terrace ca 1km of distance from the Russian hut in the sparse tundra with ridge vegetation. Around each trap vegetation sampling and record of species was carried out following the sampling protocol of Pollen monitoring programme. Moss sample was sampled as well to get recent pollen spectra. Next year, the content of the trap will be taken out and analysed for pollen and replaced for the new one for next season.

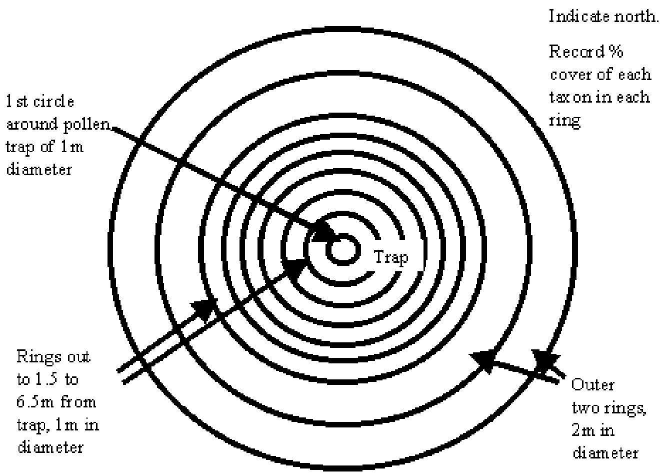

Fig. 3.5.3. Projection of vegatation mapping strategy. Image from http://www.pollentrapping.net/.

Fig. 3.5.4. Installed pollen trap.

Zoology and Parasitology

3.5.5.Zoology and parasitology

Oleg Dittrich, Eva Myšková & Tomáš Tyml

Group of parasitologists continued with examination of marine invertebrates and fish for parasites. The most common fishes (e.g. *Myoxocephalus scorpius*, *Gymnocanthus tricuspis*, *Clupea harengus* and *Boreogadus saida*) were caught using gill nets laid in littoral zone and various macrozoobenthos (e.g. *Buccinum* spp., *Mya truncata*, spirorbid polychaete and *Strongylocentrotus* spp.) were sampled during scuba diving in Billefjorden (Table 3.6.1., Fig. 3.6.1.).

Table 3.6.1. Number of dissected fish and invertebrates.

Number of dissected fish		Number of dissected invertebrates	
Myoxocephalus scorpius	66 ex.	Gammaridae	49 ex.
Clupea harengus	25 ex.	*Buccinum undatum*	41 ex.
Boreogadus saida	25 ex.	*Buccinum glaciale*	25 ex.
Gymnocanthus tricuspis	21 ex.	*Mya truncata*	18 ex.
Lumpenus lampretaeformis	11 ex.	*Hiatella arctica*	9 ex.
Gadus morhua	8 ex.	*Littorina saxatilis*	7 ex.
Mallotus villosus	8 ex	*Coleus kroyeri*	4 ex.
Hippoglossoides platessoides	2 ex.	*Buccinum polare*	3 ex.
Eumitremus sp.	2 ex.	*Astarte rugosa*	3 ex.
Liparis sp.	1 ex.	*Serripes groenlandica*	3 ex.
		Euspira pallid	2 ex.
		Chlamys islandica	2 ex.
		Margarites olivaceus	1 ex.

Fig. 3.6.1. Shell of *Coleus kroyeri.*

A significant progress has been made in study of *Podocotyle* (opecoelid trematode) life cycle. Several experiments were performed with second hosts (amphipods of genera *Gammarus* and *Onisimus*) to determine the infection way (Figs. 3.6.2. and 3.6.3.).

Fig. 3.6.2. *Onisimus*, one of the amphipod genera used in experiments with *Podocotyle.*

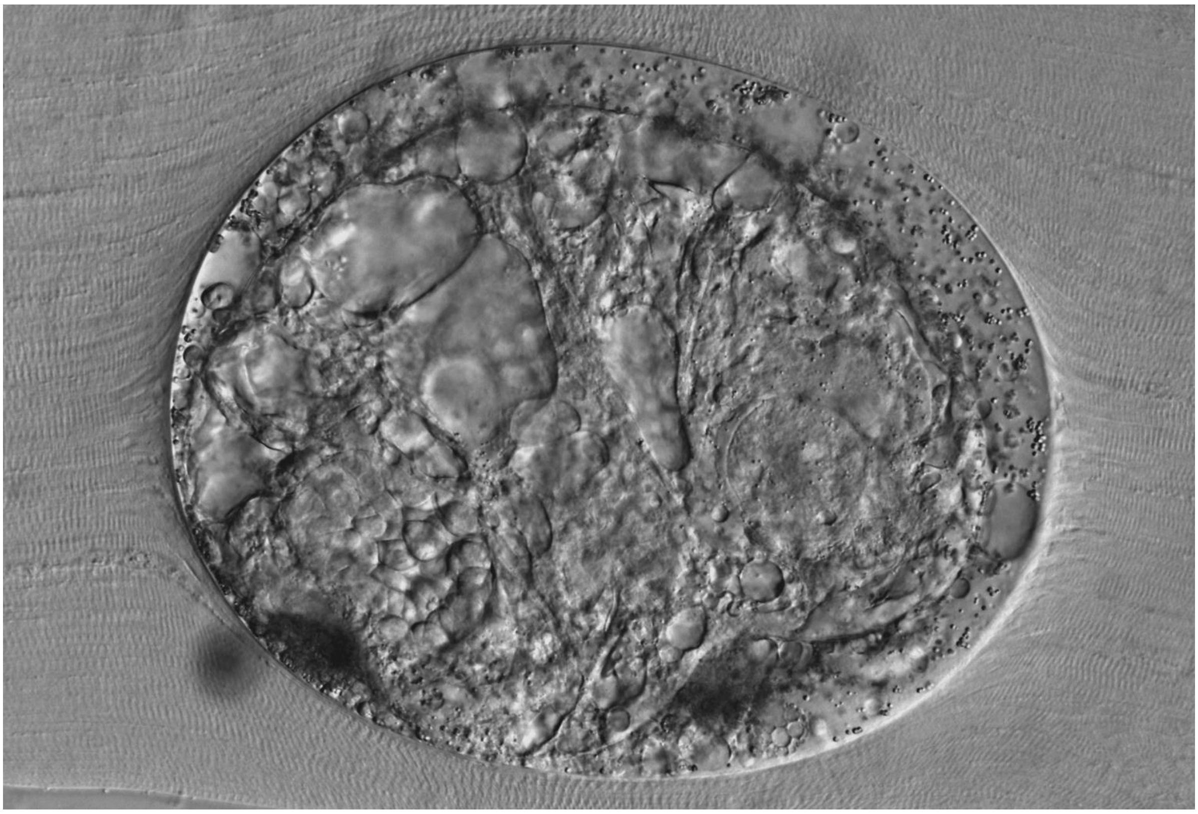

Fig. 3.6.3. Metacercaria of *Podocotyle* encysted in muscle tissue.

Blood smear preparations were made from fish blood. A few of sculpins *Myoxocephalus scorpius* were found to be infected by hemogregarine parasite, likely *Desseria myoxocephali*.

Iva Pospíšilová, master student of Oleg Ditrich, efforts to obtain the sequences of gene for SSU rRNA (Fig. 3.6.4.).

Fig. 3.6.4. Sculpin *Myoxocephalus scorpius*, host of hemogregarine parasite (likely *Desseria myoxocephali*), a leech (above the pectoral fin) should be a vector of *D. myoxocephali.*

We found trematode larval stages in rough periwinkles, *Littorina saxatilis*. We obtained enough material for morphological and molecular characterization which will help us link the larvae to adult stages (Fig. 3.6.5.).

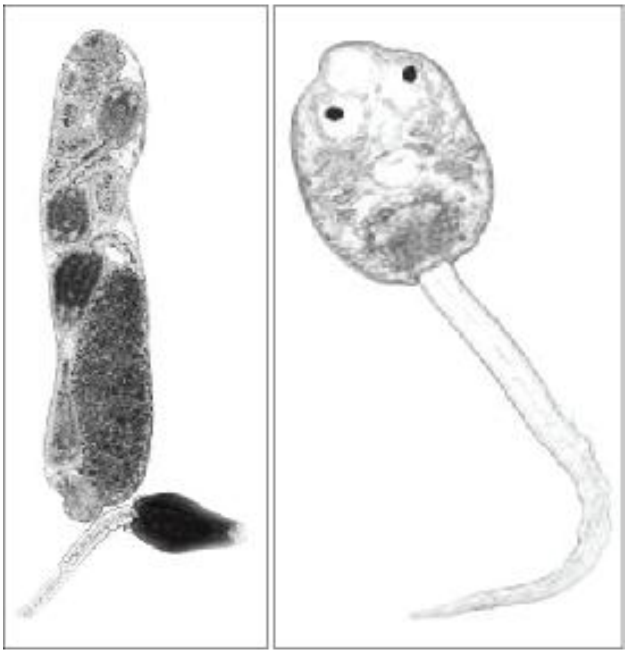

Fig. 3.6.5. Redia and cercariae from *Littorina saxatilis.*

Eva Myšková collected extensive number of material for her master thesis. She studies intestine parasites of terrestrial vertebrates in harsh condition of high Arctic and she obtained samples from animal droppings using flotation methods (Fig. 3.6.6.).

Fig. 3.6.6. Svalbard reindeer (*Rangifer tarandus platyrhynchus*), one of the target species of Eva.

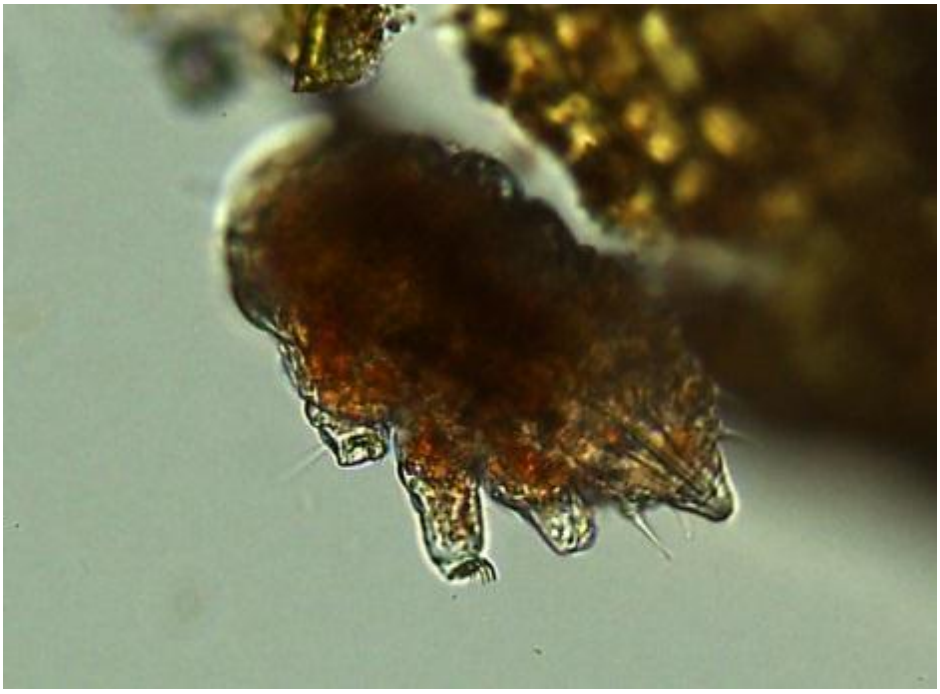

Fig. 3.6.7. A cute and brightly colored limnoterrestrial tardigrade of the order Echiniscoidea.

Microscopic invertebrates represent an important component of aquatic and limnoterrestrial biota; in particular, such organisms are quite abundant in marine benthos, terrestrial moss, lichens and soil of Arctic polar zone. Since they are highly tolerant to the wide range of natural conditions and can be transported by wind, water and vertebrates over huge distances, cosmopolitanism and absence of distribution patterns was predicted for such animals – up to the extremity that some researchers were using keys composed from studies on Europe to identify species in the Southern Hemisphere. Checking samples from many localities all over the world, we have found a number of new species, and also some specific distribution patterns of Rotifera and Tardigrada (Fig. 3.6.7.), allowing us to think that even for microbes exist biogeographical rules similar to ones observed on macrobes - the polar communities being not quite the same as such in the zones with warmer climate. It seems that everything is quite not everywhere in the microscopic world! Therefore, the goal of our team was to study microscopic fauna present on Svalbard, its diversity and distribution over the latitudinal, altitudinal and ecological gradients – and to compare the data on Arctic biota with such of the lower latitudes. In spite of that preliminary species lists of microscopic animals of Svalbard were already made, we consider them quite incomplete; also, no data on Petunia bay, except of the recent efforts of Dr M. Devetter, exist.

During two weeks between August 2 and 14, 2013 our team collected 76 samples of sea bottom sediments (depth 5, 10 and 20 m), cryoconites (small water reservoirs in glacier ice), terrestrial mosses, lichens and soil in Petunia Bay and vicinity - Adolf bay, Skans bay, Wordiekammen mountains, Nordenskiold, Sven and Ferdinand glaciers. The terrestrial samples were taken at altitudes from 0 to 746 m a.s.l., thus also representing an altitudinal gradient. Water and sediment samples, as well as some moss patches, were processed immediately after collection, using microscopes with total magnification x40 – x400. The rest of material was dried out under room temperature for subsequent investigation in the laboratory of University of Ostrava. Rotifers that were observed in the samples were identified to species; other organisms (mites, nematodes, tardigrades, gastrotrichs) were photographed and preserved in ethanol for the later examination on constant slides, since their identification is not possible in the field conditions.

Even the preliminary observation of samples gave inspiring results: in spite of that 170 species of rotifers (circa 12% of European fauna) are already known from Svalbard, in 11 preliminary observed samples we have found 17 species, including 4 taxa new for Svalbard fauna – *Adineta acuticornis*, *Habrotrocha crenata crenata* (Fig. 3.6.8.), *H. gracilis*, *Macrotrachela quadricornifera rigida*. Besides these, we have found a rotifer - obviously not an abnormal, but a healthy individual, - which features do not correspond to any known description, thus suggesting a potential new species for science record from Svalbard. If it is so, this species will be the first bdelloid rotifer first described from Arctic. Another potentially new taxon may be the one identified as *Macrotrachela* (*conformis*) *musculosa*, a red-colored rotifer inhabiting exclusively cryoconites (Fig. 3.6.9.).

Fig. 3.6.8. *Habrotrocha crenata crenata* – a rotifer species not previously recorded in Svalbard.

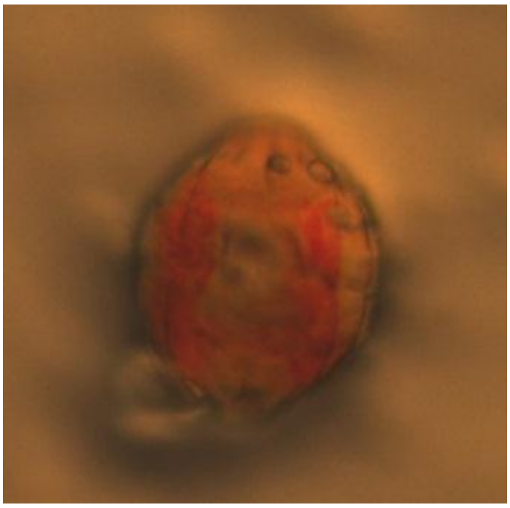

Fig. 3.6.9. *Macrotrachela* cf *musculosa* (contracted) – a rotifer living in cryoconites.